The Nature of a Sodium–Crown Interaction studied by Sodium-23 Nuclear Magnetic Resonance and by Crystal Structure Determination of a Complex with Co-ordinated Solvent *

Joyce C. Lockhart, Martin B. McDonnell, William Clegg, M. N. Stuart Hill, and Martin Todd
Department of Inorganic Chemistry, The University, Newcastle upon Tyne NE1 7RU

New measurements were obtained by n.m.r. methods on the relaxation times of ^{23}Na nuclei in ligand–metal salt solutions in pyridine–CH_2Cl_2 (1 : 1) with the intention of modelling the rate processes in ion selective electrodes. Cation-exchange rates for some propeller crowns suggest the mechanism of Na exchange in the presence of excess sodium ions is dissociative. Sodium exchange rates are slower for more rigid propeller crowns. The solvated species are shown by means of a crystal structure to contain only one pyridine co-ordinated to sodium, but additional molecules of solvating pyridine are present in the crystal, and evident in elemental analyses. An additional sodium-containing species was discovered at temperatures of 230 K and below in this solvent. Results are of significance in relation to understanding the nature of cation–ionophore interaction in ion-selective electrodes and other selective devices.

At Newcastle, we are investigating the fundamental mechanism of selectivity[1-3] in ion-selective electrodes, concentrating particularly on the K/Na selectivity of valinomycin and the crown ethers in typical poly(vinyl chloride) (pvc) configurations. The problem has been approached through impedance measurements on the typical pvc membrane which can profile certain steps at the interface.[3] Here we present a kinetic approach to sodium exchange with propeller[4] crowns (dinaphthopolycycloalkins), L.

$$M^+(solv) + L \underset{k_{-1}}{\overset{k_1}{\rightleftharpoons}} ML^+ + solv \quad (1)$$

$$ML^+ + {}^*M^+ \underset{}{\overset{k_2}{\rightleftharpoons}} {}^*ML^+ + M^+ \quad (2)$$

$$^*L + ML^+ \rightleftharpoons M^*L^+ + L \quad (3)$$

Measurements have been made in a single homogeneous phase, to establish kinetics of processes which might have a place at the interface or in the membrane [equations (1)—(3)]. In the electrode, processes (1) and (2) may take place at the membrane surface, processes (2) and (3) may take place in the membrane interior. Our original intention was to look at these processes in solvents chosen to simulate a real membrane, using for example a typical plasticiser,[5] with a halogeno carbon to simulate the pvc. However, typical plasticisers such as dibutyl phthalate and dioctyl sebacate, while they dissolved the materials even at the concentrations and temperatures required for this study, gave very wide n.m.r. lines. After considering and rejecting many solvent combinations, we chose the polar solvent pyridine (py), to mimic the plasticiser, admixed with dichloromethane, to represent the pvc.

The quadrupolar nuclei ^{23}Na and ^{39}K (both of spin quantum number $I = \frac{3}{2}$) have been used for the analysis of the kinetics of alkali cation exchange[6-11] in ligand–metal systems [although the method is restricted to systems containing excess alkali cations, so that the process in equation (3) is unlikely to be significant]. The kinetic data obtained are usually at temperatures less than 0 °C (see later). Shchori *et al.*[6,7] suggested that exchange went through two possible mechanisms,

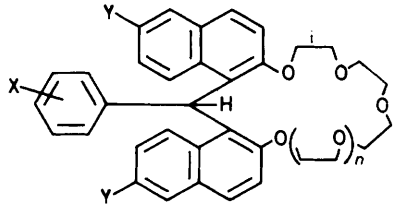

L	X	Y	n
(1)	2-F	H	1
(2)	2,6-Cl_2	Bu^t	1
(3)	3,5-Me_2	Bu^t	2
(4)	3,4,5-$(MeO)_3$	Bu^t	1
(5)	2-MeO	H	1
(6)	3,4,5-$(MeO)_3$	Bu^t	2

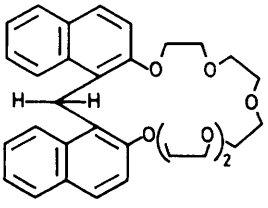

(7)

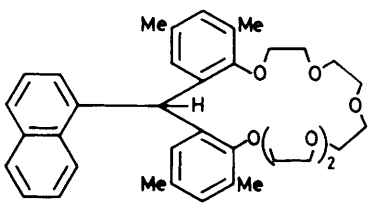

(8)

* *Supplementary data available:* see Instructions for Authors, *J. Chem. Soc., Dalton Trans.*, 1989, Issue 1, pp. xvii—xx.

Non-S.I. unit employed: cal = 4.184 J.

Table 1. Analysis of pyridine solvates* of $NaBPh_4$–crown complexes, $NaBPh_4$·L·$(py)_m$

		Found (%)			Calc. (%)			
L	*m*	C	H	N	C	H	N	Formula
(**2**)	1	75.2	6.1	1.05	76.1	6.5	1.2	$C_{72}H_{73}BCl_2NaNO_5$
(**2**)	2	75.5	5.8	2.6	76.1	6.5	2.3	$C_{77}H_{78}BCl_2NaN_2O_5$
(**2**)	2	73.2	6.1	2.1	73.3	6.3	2.2	$C_{77}H_{78}BCl_2NaN_2O_5$·$0.5CH_2Cl_2$
(**2**)	3	75.1	6.1	3.1	76.0	6.5	3.2	$C_{82}H_{83}BCl_2NaN_3O_5$
(**3**)	3	78.2	6.7	2.9	78.5	7.1	3.2	$C_{86}H_{93}BNaN_3O_6$·$0.25CH_2Cl_2$
(**4**)	2	77.3	6.8	2.15	77.7	7.0	2.3	$C_{80}H_{86}BNaN_2O_8$
(**6**)	1	76.2	7.0	0.95	77.0	7.0	1.2	$C_{77}H_{83}BNaNO_8$·$0.25CH_2Cl_2$
(**7**)	2	76.2	6.2	2.8	76.5	6.4	2.7	$C_{65}H_{64}BNaN_2O_6$·$0.25CH_2Cl_2$

* Pyridine solvates obtained from the contents of n.m.r. tubes.

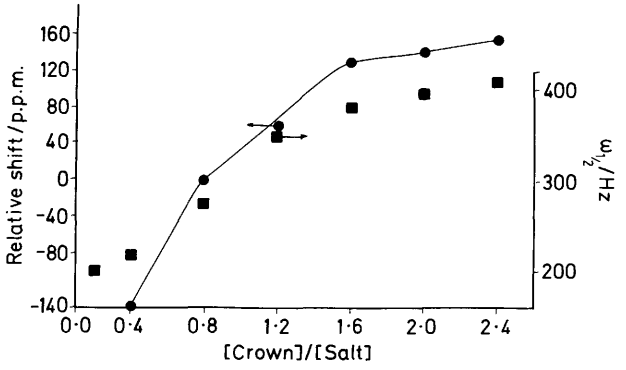

Figure 1. Variation of chemical shift or linewidth *versus* [crown]/[salt] for solutions of propeller crown (**1**) and a constant concentration of $NaBPh_4$ (0.1 mol dm^{-3}) in pyridine–CD_2Cl_2 (1:1) at 297 K

a dissociative one [reverse of equation (1)] and an associative mechanism, that shown in equation (2). On the assumption that equations (1) and (2) represent the sole operative mechanisms in cation exchange, equation (4) may be derived (as proposed by Shchori *et al.*[6,7]) for the dissociative mechanism [reverse of equation (1)] and the bimolecular exchange mechanism [shown in equation (2)]. Supposing these two mechanisms may each contribute to the overall rate of exchange, the reciprocal mean lifetime of the solvated cation may be expressed by equation (4), where [B] is the concentration of complexed

$$1/\tau = k_2[B] + k_{-1}[B][solv]/[A] \quad (4)$$

Na, and [A] is the concentration of solvated cation. The contribution of the two mechanisms may be obtained by plotting $1/\tau[B]$ *vs.* $1/[A]$, the intercept being equal to the bimolecular exchange rate constant, k_2[equation (4)] and the gradient equal to the apparent dissociative rate constant, $k_{-1}(=k_{-1}[solv])$. The results of Shchori *et al.*[6,7] suggested that the dissociative mechanism was predominant, and the associative one negligible for dibenzo-18-crown-6 (6,7,9,10,17,18,20,21-octahydrodibenzo[*b*,*k*][1,4,7,10,13,16]hexaoxacyclo-octadecine) and sodium ions, but a number of papers subsequently reported evidence for associative and other mechanisms.[9–11] Access to high-field n.m.r. facilities has enabled us to explore the systems described above in some depth, and the fortunate crystallisation of suitable crystals enabled us to consider the structure of the solvated species. These are more complex than hitherto realised.

Experimental

Materials.—Ligands were obtained as described previously.[2,4] Sodium tetraphenylborate (Fluka) was recrystallised from distilled AnalaR acetone and dried under vacuum before use. N.m.r. solvents were dried before use. Crystals were often isolated from deposits in n.m.r. tubes. Typical analyses for these are shown in Table 1.

N.M.R. Measurements.—Data for ^{23}Na (100%, $I = \frac{3}{2}$) were obtained on a Bruker WM300WB at 79.35 MHz and on a Bruker HFX90 instrument at 23.8 MHz. We sought, but did not find, the alkahest for all alkali tetraphenylborates and propeller crown combinations at low temperatures. The solvent actually used was a 2:1:1 mixture of pyridine–CH_2Cl_2–CD_2Cl_2, which had a liquid range down to −120 °C, and retained crowns and sodium salts in solution as low as −100 °C; it did not dissolve potassium salts under those conditions, so we were unable to make the K/Na comparison we would have wished. Where possible, a solution of NaCl in D_2O in a capillary tube was the external reference. This was not viable at low temperatures, when the reference used was free $NaBPh_4$ in a solvent with low freezing point. Often the reference signal overlapped those for the solutions of interest, and had to be omitted. Solutions of $NaBPh_4$ with ligand (**1**) of L:M mole ratio from 0.0 to 2.0 were examined; plots of linewidth ($\Delta\nu_{\frac{1}{2}}$) and shift *versus* mole ratio are shown in Figure 1, suggesting that a weak 1:1 complex was formed, and that some further aggregation to a weaker 2:1 or higher complex may occur. It should be noted that the linewidth was several hundred Hz for these complexes. The lifetime $1/\tau_A$ of a solvated sodium ion was calculated from the transverse relaxation time $1/T_2$ of the sodium nuclei, obtained from linewidth measurements ($\Delta\nu_{\frac{1}{2}} = 1/\pi T_2$). A comparison was made of $1/T_1$ and $1/T_2$ for a solution of salt in solvent. These were in satisfactory agreement indicating the sodium spectra studied were in the extreme narrowing region.

Dilution Experiment.—The kinetics were usually measured at a fixed concentration of sodium salt, while the concentration of the crown was varied.[10] In two cases [ligands (**4**) and (**6**)] we tested the variation of rate constant for a series of solutions with a [Na]:[L] fixed ratio of 4:1, and a total [Na] of 0.2, 0.0022, and 0.000 88 mol dm^{-3} respectively, and at 300 K, in the fast-exchange region of the *Z* curve. For a bimolecular mechanism,[11] the rate constants should decrease with dilution of the sample, which at 300 K should lead to wider lines. In fact the linewidths actually narrow on dilution, as expected for a unimolecular mechanism, with variation in solute composition.

Crystal Data for Pyridinated Complex of Crown (**4**), $[Na(py)(C_{46}H_{56}O_8)][BPh_4]$·py, M = 1237.4, monoclinic, a =

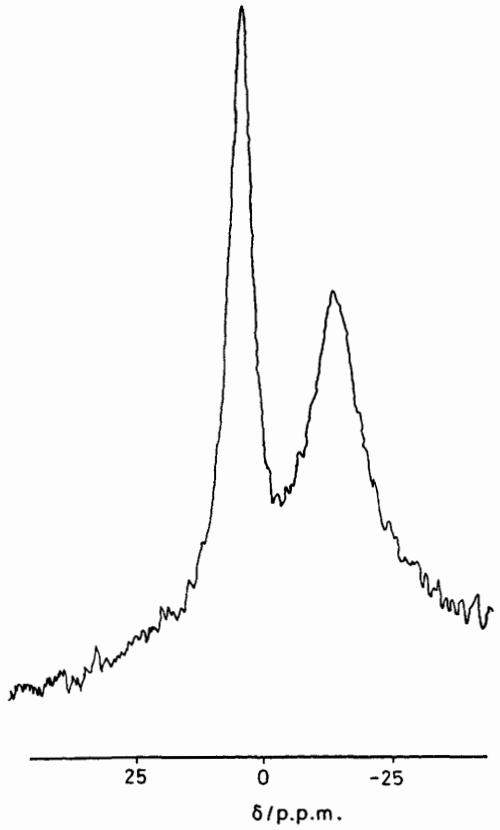

Figure 2. The two sodium signals separated at 225 K for propeller crown (**2**) (0.067 mol dm^{-3}) and $NaBPh_4$ (0.2 mol dm^{-3}) in pyridine–CD_2Cl_2 (1:1)

17.696(2), b = 14.168(1), c = 28.433(2) Å, β = 97.39(1)°, U = 7 069.4 $Å^3$ (from 2θ values of 32 reflections, 20—40°), Z = 4, D_c = 1.162 g cm^{-3}, $F(000)$ = 2 640, space group $P2_1/n$. 9 504 Reflections were measured with a Siemens AED2 diffractometer and graphite-monochromated Cu-$K\alpha$ radiation (λ = 1.541 84 Å) from a crystal of size 0.3 × 0.3 × 0.4 mm in a Lindemann capillary ($2\theta_{max.}$ = 110°, ω/θ scan from 0.68° below α_1 to 0.68° above α_2, 14—56 s per reflection). Three periodically measured standard reflections showed no significant variations. Absorption corrections were not applied (μ = 0.60 mm^{-1}). Of the 8 866 unique reflections (R_{int} = 0.029), 5 349 with $F > 3\sigma(F)$ were used for structure determination by automatic direct methods and blocked-cascade least-squares refinement on F.[12] The phenyl groups of the anion were constrained as regular hexagons with C–C = 1.395 Å; H atoms were included at calculated positions, to give C–H = 0.96 Å, H–C–H = 109.5°, aromatic H on ring angle external bisectors, $U(H) = 1.2U_{eq}(C)$. Hydrogen atoms were not included for the unco-ordinated pyridine molecule, in which all ring atoms were refined as carbon. Anisotropic thermal parameters were refined for all non-hydrogen atoms. An isotropic extinction parameter x = 3.0(2) × 10^{-6} was employed to give $F_c' = F_c/(1 + xF_c^2/\sin 2\theta)^{\frac{1}{4}}$. The weighting scheme[13] was $w^{-1} = \sigma^2(F) + 32 - 293G + 879G^2 - 43S + 29S^2 + 39GS$, where $S = \sin\theta/\sin\theta_{max.}$ and $G = F_o/F_{max.}$. Final residuals were R = 0.097, $R' = (\Sigma w\Delta^2/\Sigma wF_o^2)^{\frac{1}{2}}$ = 0.042 for 782 parameters, goodness of fit = 1.23. A final difference synthesis contained no significant features. Atomic scattering factors were taken from ref. 14.

Additional material available from the Cambridge Crystallographic Data Centre comprises H-atom co-ordinates, thermal parameters, and remaining bond lengths and angles.

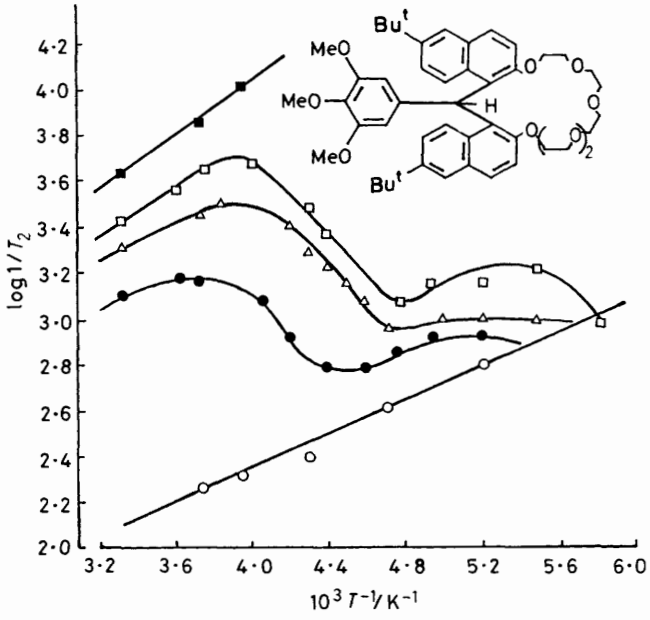

Figure 3. Z Curve plots for ^{23}Na n.m.r. signals for $NaBPh_4$ (0.2 mol dm^{-3}) containing: ○, no propeller crown; ●, 0.054; △, 0.1; □, 0.133; and ■, 0.2 mol dm^{-3} propeller crown (**6**) in pyridine–CD_2Cl_2 (1:1)

Results and Discussion

N.m.r. parameters were obtained for sodium ions in solution with a deficit of ligand; those used were (**1**)—(**4**), (**7**), and (**8**). In systems where most potential donors are oxygens, there is very little shift difference between solvated and complexed cation. However, departures from cubic symmetry for the complexed cation ensure that the linewidths are very different. It is usual for such sodium n.m.r. studies that the spectra consist of one line, with little or no shift variation, and variations in the linewidth alone may be interpreted to provide kinetic information. In the fast exchange limit, a weighted average linewidth $1/T_{2(av)}$ is observed. In the slow exchange limit, two lines, a narrow one due to solvated cation, and a very wide one due to complexed cation should be superposed. In practice, the line for the complexed cation is too wide for normal observation and only the narrow one is usually observed. We have a slightly more complicated situation here. For most propeller crowns in this solvent system, and at temperatures of 208 K and below, the supposed 'narrow' line for the solvated cation is split further into two lines; the exceptions are crown (**2**) (see Figure 2) for which the separation of the second line is at a higher temperature 230 K, and crown (**3**), for which the second signal seems to consist of two overlapping additional lines, which cannot be resolved. An interpretation of these observations and of the low temperature exchange process is made later. Since this second exchange process is essentially complete at 210 K [or 230 K for crown (**2**)] and above, the time-averaged narrow signal at *ca.* 210 (230) K was taken to represent the signal of 'solvated' cation, for the purposes of applying equation (4) to derive the kinetics. Results for the higher temperature exchange process for ligand (**6**) are displayed in Figure 3 as typical Z plots of log $1/T_2$ *versus* reciprocal temperature. In the fast exchange region, the linewidth of the observed signal is a population average. In the intermediate region the rate of exchange is of the order of the relaxation rate, and the lifetime of the solvated species can be determined from equation (5), where $1/T_{2(av)} = P_A/T_{2A} +$

$$1/\tau_A = \frac{(1/T_{2B} - 1/T_2)(1/T_2 - 1/T_{2A})P_B}{[1/T_{2(av)} - 1/T_2]} \quad (5)$$

Table 2. Kinetics of Na^+ exchange between $NaBPh_4$ and crown ethers[a]

Crown[b]	[Crown]/mol dm^{-3}	$1/\tau$[c]/s^{-1}	T(K)	E_a[d]/k cal mol^{-1}	k_{-1} (solv.)[e]/s^{-1}	$1/\tau$ at 300 K/s^{-1}
(**2**) (285)	0.065	236	241	8.7	3 364 (260)	0.75×10^4
(**2**) (290)	0.1	555	241	9.3		2.64×10^4
(**3**) (280—90)	0.06	660	241	4.0		
(**4**) (260)	0.05	1 278	241	5.1		1.14×10^4
(**4**)	0.09	3 788	241	5.5	4 514 (241)	3.66×10^4
(**6**) (260)	0.054	1 168	238	7.9		3.74×10^4
(**6**)	0.133	5 570	238	6.2	3 006 (238)[f]	8.45×10^4
(**7**) (260)	0.073	758	241	12.3		12.2×10^4
(**7**)	0.11	3 647	241	9.8		19.7×10^4

[a] $NaBPh_4$ 0.2 mol dm^{-3} in py–CH_2Cl_2 (1 : 1). [b] Turning temperature (K) of Z curve in parentheses. [c] Calculated from equation (5). [d] Arrhenius energy for $1/\tau$ value. [e] Temperature (K) in parentheses. [f] $\Delta G^{\ddagger} = 10$ kcal mol^{-1}; *cf.* propeller flip has $\Delta G^{\ddagger} = 11.3$ kcal mol^{-1}.

Table 3. Atomic co-ordinates ($\times 10^4$) for $[Na(py)(C_{46}H_{56}O_8)][BPh_4]\cdot py$

Atom	x	y	z	Atom	x	y	z
Na	2 091(1)	2 235(2)	512(1)	C(46)	1 112(3)	4 945(5)	−197(2)
O(1)	3 223(2)	2 861(2)	980(1)	C(47)	4 157(3)	8 339(4)	1 070(2)
C(2)	3 577(4)	2 196(5)	1 321(2)	C(48)	3 641(4)	8 889(4)	694(2)
C(3)	3 035(5)	1 516(5)	1 447(3)	C(49)	4 990(3)	8 569(4)	1 023(2)
O(4)	2 639(3)	1 068(3)	1 053(2)	C(50)	3 985(5)	8 658(4)	1 552(2)
C(5)	2 059(4)	419(5)	1 181(3)	C(51)	7 342(4)	2 074(5)	1 071(3)
C(6)	1 639(4)	68(5)	733(3)	C(52)	7 548(4)	1 052(6)	1 035(5)
O(7)	1 250(3)	825(3)	508(2)	C(53)	7 824(4)	2 578(9)	739(5)
C(8)	878(6)	597(8)	31(4)	C(54)	7 560(6)	2 436(10)	1 544(4)
C(9)	1 252(6)	899(6)	−325(4)	B	923(4)	8 155(5)	1 983(2)
O(10)	1 511(4)	1 809(4)	−277(2)	C(56)	549(2)	9 779(4)	2 354(1)
C(11)	1 948(4)	2 090(6)	−634(2)	C(57)	236	10 683	2 332
C(12)	2 764(3)	1 909(5)	−514(2)	C(58)	−104	11 045	1 899
O(13)	3 010(2)	2 279(2)	−51(1)	C(59)	−129	10 501	1 489
C(14)	3 767(3)	2 137(4)	115(2)	C(60)	185	9 597	1 510
C(15)	4 211(3)	2 886(3)	292(2)	C(55)	524	9 235	1 943
C(16)	3 935(3)	3 905(3)	255(1)	C(62)	−18(2)	7 740(3)	2 629(2)
C(17)	3 684(2)	4 321(3)	709(1)	C(63)	−366	7 105	2 909
C(18)	3 398(3)	3 817(3)	1 051(2)	C(64)	−253	6 137	2 862
C(19)	3 199(3)	4 213(4)	1 468(2)	C(65)	208	5 804	2 535
C(20)	3 309(3)	5 138(4)	1 550(2)	C(66)	555	6 440	2 255
C(21)	3 604(3)	5 727(3)	1 213(2)	C(61)	442	7 408	2 302
C(22)	3 729(3)	6 704(4)	1 297(2)	C(68)	229(2)	7 445(3)	1 176(2)
C(23)	4 014(3)	7 291(4)	982(2)	C(69)	201	7 154	706
C(24)	4 164(3)	6 870(3)	557(2)	C(70)	869	7 116	493
C(25)	4 056(3)	5 940(3)	460(2)	C(71)	1 564	7 368	752
C(26)	3 786(3)	5 320(3)	791(1)	C(72)	1 591	7 659	1 222
C(27)	4 043(3)	1 210(4)	145(2)	C(67)	923	7 698	1 435
C(28)	4 764(3)	1 023(4)	347(2)	C(74)	2 199(3)	9 108(3)	2 326(1)
C(29)	5 258(3)	1 753(3)	537(2)	C(75)	2 953	9 153	2 540
C(30)	6 010(3)	1 560(4)	720(2)	C(76)	3 350	8 325	2 673
C(31)	6 509(3)	2 243(5)	895(2)	C(77)	2 993	7 451	2 592
C(32)	6 212(3)	3 171(4)	886(2)	C(78)	2 239	7 406	2 379
C(33)	5 479(3)	3 383(4)	717(2)	C(73)	1 842	8 234	2 246
C(34)	4 967(3)	2 688(3)	518(2)	N(79)	1 214(3)	3 305(4)	863(2)
C(35)	3 395(3)	4 142(3)	−193(2)	C(80)	1 337(4)	4 205(6)	972(2)
C(36)	3 682(3)	4 094(4)	−624(2)	C(81)	834(4)	4 769(6)	1 161(2)
C(37)	3 214(3)	4 309(4)	−1 040(2)	C(82)	171(5)	4 396(7)	1 250(3)
C(38)	2 463(3)	4 587(4)	−1 029(2)	C(83)	8(4)	3 488(6)	1 145(3)
C(39)	2 188(3)	4 643(4)	−594(2)	C(84)	549(4)	2 944(5)	955(3)
C(40)	2 654(3)	4 435(3)	−180(2)	C(85)	8 211(6)	9 357(7)	2 312(3)
O(41)	3 439(2)	4 296(3)	−1 484(1)	C(86)	8 185(6)	8 858(9)	1 918(4)
C(42)	4 214(4)	4 116(6)	−1 524(2)	C(87)	7 569(6)	8 509(9)	1 706(3)
O(43)	1 999(2)	4 812(3)	−1 445(1)	C(88)	6 973(6)	8 543(13)	1 900(4)
C(44)	1 603(4)	4 043(6)	−1 677(2)	C(89)	6 882(6)	9 026(11)	2 294(5)
O(45)	1 443(2)	4 913(3)	−623(1)	C(90)	7 548(6)	9 247(9)	2 502(3)

P_B/T_{2B}; $1/T_{2A}$ and $1/T_{2B}$ are the relaxation rates of the free and complexed Na^+, while P_A and P_B are the fractions of free and complexed Na^+. In the fast exchange limit, $1/T_2 = 1/T_{2(av)}$, and the extrapolation of this curve is used to obtain $1/T_{2(av)}$ in the intermediate region. In the slow exchange region, $1/T_2 = 1/T_{2A}$ and the extrapolation of this curve is used to obtain $1/T_{2A}$ in the intermediate region.

The variation in linewidth with temperature of two solutions containing 0.05 and 0.09 mol dm^{-3} trimethoxy crown (**4**) together with 0.2 mol dm^{-3} $NaBPh_4$ was analysed to provide

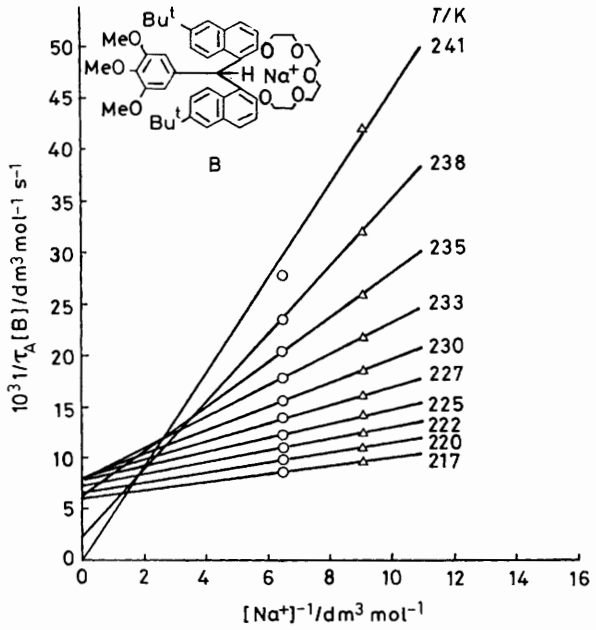

Figure 4. Plot of $1/\tau_A[B]$ *versus* $1/[Na^+]$ [test of equation (4)] over a temperature range for propeller crown (**4**) and $NaBPh_4$ mixtures

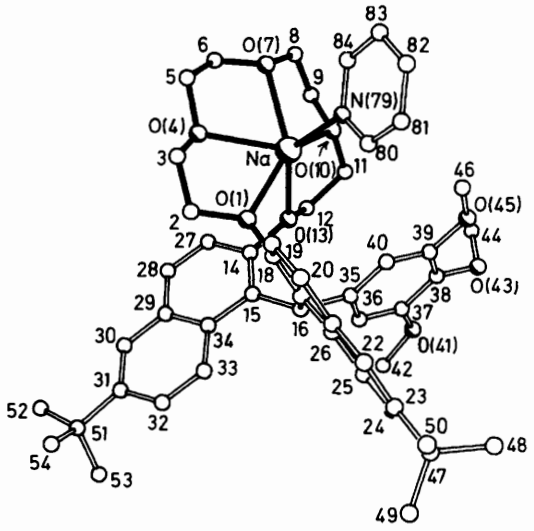

Figure 5. Structure of the cation of $[Na(py)(C_{46}H_{56}O_8)][BPh_4]\cdot py$. Carbon atoms are labelled by their numbers only. Filled bonds indicate the ether strand and Na co-ordination

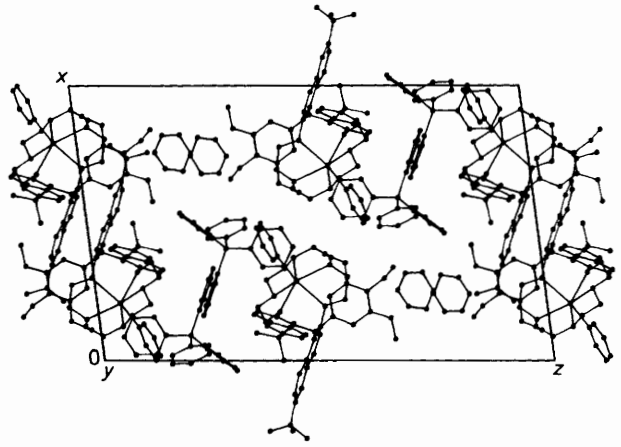

Figure 6. The packing of $[Na(py)(C_{46}H_{56}O_8)][BPh_4]\cdot py$, seen in parallel projection along the *b* axis

lifetimes ($1/\tau_A$) for the solvated sodium cation by the method described by Shchori *et al.*[6,7] and Shporer and Luz[8] (assuming that in the intermediate exchange region, the formation of the stacked species is not significant). An Arrhenius plot of $1/\tau_A$ against $1/T$ provided apparent activation energies of 5.1 and 5.5 kcal mol^{-1}. These values are unrealistically low for a single mechanism to be operative. Supposing the exchange of Na between the solvated and complexed sites to proceed *via* two mechanisms as proposed by Shchori *et al.*[6,7] the contribution of the two mechanisms could be obtained graphically, as shown in Figure 4, for the two concentrations of trimethoxy crown (**4**) at a number of temperatures. Qualitatively it may be seen that the dissociative mechanism is predominant at higher temperatures, while the bimolecular exchange may become more important at low temperatures. In a dilution experiment (see Experimental section) at 300 K there was no evidence for a bimolecular exchange.

For other cation–ligand combinations [crowns (**2**), (**4**), (**6**), and (**7**)], the set of observed exchange rate constants ($1/\tau_A$), at different temperatures, when plotted according to the Arrhenius relation, gives activation energies as shown in Table 2. This Table lists also the turning temperatures of the *Z* curves. For the propeller ligands (**2**) and (**3**), it may be seen that the sodium exchange is slower than for the other ligands. Exchange rates at comparable temperatures are included in Table 2. The differences in rate between different propeller crowns are small (within a factor of 10 at 240 K), but there is a definite trend, with rates for the most rigid crowns being less than for the more flexible ones. The Shchori test of mechanism was also applied, for several of these crowns, and again the dissociative mechanism appeared in the higher temperature region, thus being the mechanism most likely to be important in the operation of the ion-selective electrode. The outcome for K/Na selectivity will depend also on relative rates of K exchange, which we were unable to obtain in this work.

Nature of the Complexed Species.—N.m.r. tubes containing ligand and $NaBPh_4$ in pyridine–CH_2Cl_2 (1:1) deposited large clear crystals, after 2 years in a refrigerator. These on filtration were found to contain pyridine, which was readily liberated to the atmosphere, with resultant break up of the crystal. A number of these deposits were crushed and vacuum dried before analysis. They contained varying amounts of pyridine, often not a stoicheiometric ratio, suggesting that some of the pyridine was loosely bound. However, the calculated percentages of C and H were almost the same, whether one, two, or three molecules of pyridine were present, so that the very low percentage of N (1—3%) was the main criterion of composition. Some analyses are shown in Table 1. *X*-Ray investigation of several crystals generally indicated disorder, but one example [complex of ligand (**4**)] was found to be suitable for *X*-ray analysis. The atomic co-ordinates are in Table 3. The compound was found to contain sodium, co-ordinated to one mole of pyridine, and to the five cyclic ether oxygens of ligand (**4**). This cation was packed in a lattice containing also one mole of free pyridine and one tetraphenylborate anion per sodium. The unit cell contained four such aggregates. The structure of the complexed cation is shown in Figure 5, and a packing diagram is shown in Figure 6. Selected geometrical parameters are shown in Table 4. Several features of this structure are notable,

Table 4. Selected bond lengths (Å), bond angles (°) and torsion angles (°) for $[Na(py)(C_{46}H_{56}O_8)][BPh_4]\cdot py$

Na–O(1)	2.424(4)	Na–O(4)	2.378(5)
Na–O(7)	2.490(5)	Na–O(10)	2.422(5)
Na–O(13)	2.425(4)	Na–N(79)	2.471(7)
O(1)–Na–O(4)	70.2(1)	O(1)–Na–O(7)	138.3(2)
O(4)–Na–O(7)	68.8(2)	O(1)–Na–O(10)	145.2(2)
O(4)–Na–O(10)	121.0(2)	O(7)–Na–O(10)	67.3(2)
O(1)–Na–O(13)	77.1(1)	O(4)–Na–O(13)	101.1(2)
O(7)–Na–O(13)	118.0(2)	O(10)–Na–O(13)	68.6(2)
O(1)–Na–N(79)	94.1(2)	O(4)–Na–N(79)	113.0(2)
O(7)–Na–N(79)	95.0(2)	O(10)–Na–N(79)	108.3(2)
O(13)–Na–N(79)	139.5(2)		
C(18)–O(1)–C(2)–C(3)	135.4(6)	O(1)–C(2)–C(3)–O(4)	53.3(8)
C(2)–C(3)–O(4)–C(5)	−176.6(6)	C(3)–O(4)–C(5)–C(6)	174.7(6)
O(4)–C(5)–C(6)–O(7)	−66.4(7)	C(5)–C(6)–O(7)–C(8)	173.4(7)
C(6)–O(7)–C(8)–C(9)	−101.4(10)	O(7)–C(8)–C(9)–O(10)	−45.6(12)
C(8)–C(9)–O(10)–C(11)	175.6(8)	C(9)–O(10)–C(11)–C(12)	−90.3(8)
O(10)–C(11)–C(12)–O(13)	−49.9(8)	C(11)–C(12)–O(13)–C(14)	178.3(5)
C(12)–O(13)–C(14)–C(15)	129.3(5)	O(13)–C(14)–C(15)–C(16)	−8.5(7)
C(14)–C(15)–C(16)–C(17)	102.0(5)	C(15)–C(16)–C(17)–C(18)	−28.3(6)
C(16)–C(17)–C(18)–O(1)	−8.0(7)	C(17)–C(18)–O(1)–C(2)	123.7(5)

in connection with the general assessment of propeller crown structure, and in the possible arrangement of the crowned cation with the tetraphenylborate anion, which is known to be a significant and useful counter ion for use in ion-selective electrode membranes.

This is the first successful crystal-structure determination of a cationic complex of a propeller crown with a non-co-ordinating anion. The distances from the sodium cation to the borons of the four nearest-neighbour tetraphenylborate anions are all greater than 7.5 Å. The packing diagram illustrates the considerable tendency of the aromatic rings to stack in parallel planes throughout the crystal. Thus the tetraphenylborates line up with one Ph ring parallel to the symmetry related ring of an adjacent tetraphenylborate (the closest B–B distances in the crystal are >9.0 Å) and also to the plane of one naphthyl from the triaryl propeller. The trimethoxyphenyl ring lies approximately in the *XZ* plane, and is found perpendicular to the first plane; also lying approximately in the *XZ* plane are one ring of each tetraphenylborate and the (disordered) loose pyridine in the channels.

That the arrangement of the propeller turns out to be the isomer most commonly observed (in seven out of the eight structures so far determined) supports the hypothesis[15] that this is the most stable propeller isomer.

The conformation of the crown ether ring is similar to that in the sodium complex of (**5**) previously published.[16] Whereas this had the sixth position of the co-ordination sphere completed by thiocyanate, in the present instance pyridine completes the co-ordination sphere. This suggests a possible co-ordinating role of the plasticiser in those ion-selective electrode membranes in which there is a tetraphenylborate counter ion and in which an ionophore does not fully complete the cation co-ordination sphere. The torsion angles round the crown ether strand in $[Na(py)(C_{46}H_{56}O_8)][BPh_4]\cdot py$ (shown in Figure 5) are ag^+a,ag^-a,ag^-a,ag^-a compared to ag^+a, ag^-a, ag^+g, ag^-a in the sodium salt of (**5**).[16]

Although unco-ordinated pyridine was found in the structure, there was no methylene chloride (but some samples analysed for a trace of methylene chloride). It is suggested by analogy that plasticiser (with donor C=O groups instead of the pyridine) is important in co-ordinating the alkali cation in ion-selective electrode membranes, while the pvc is essentially inert in relation to the structure of the complexes formed. This would not preclude some role of pvc impurities in the actual selection mechanism of an ion-selective electrode.

Table 5. Free energies of activation for exchange between two sodium sites at low temperatures*

Crown	Peak separation/ Hz (T/K)	ΔG/kcal mol^{-1} (T_c/K)
(**2**)	1 800 (200)	9.7 (235)
(**4**)	1 650 (172)	8.4 (202)
(**6**)	2 290 (180)	8.5 (208)
(**8**)	1 980 (195)	8.6 (210)

* Determined from the approximate coalescence temperature, by the method of H. Shanan-Atidi and K. H. Bar-Eli, *J. Phys. Chem.*, 1970, **74**, 961.

Low-temperature Species.—It is reasonable to assume that structural features of the monopyridine complex observed in the crystal from the n.m.r. tube, may be retained in the solution undergoing n.m.r. analysis. We next consider the structure of the species taking part in the low-temperature exchange process. The solvated complex $[Na(py)(C_{46}H_{56}O_8)][BPh_4]\cdot py$ is believed to be the main crowned cation at the temperature of fast or intermediate exchange rate. Its linewidth extrapolated to 178 K would be 26 kHz, and it would be unobservable. For each system that we studied, the sodium signal split at temperatures ranging from 230 K [for crown (**2**)] to 208 K, to give signals we suppose to be solvated cation and an unknown. The activation energy $\Delta G^{\ddagger}$ of this low-temperature process could be estimated at 8.4—9.6 kcal mol^{-1}, see Table 5, which suggests a complexation–decomplexation rather than a solvation sphere switch. The single narrow line observed in earlier low-field work[6–8] may turn out in some instances to be an oversimplification. We have found multiple lines elsewhere, *e.g.* in mixtures of dibenzo-18-crown-6 and sodium tetraphenylborate at 79 MHz, both in the pyridine–CH_2Cl_2 solvent used in this work and in an *N*-methyl-2-pyrrolidone–CH_2Cl_2 mixture. We fear such extra signals may have been missed at lower field strengths. Further experiments were designed to elucidate the phenomenon. Observations of the new low-temperature signals were made in various mixtures in which (*a*) the L:M ratio and (*b*) the ligand, (*c*) the anion, and (*d*) the temperature were

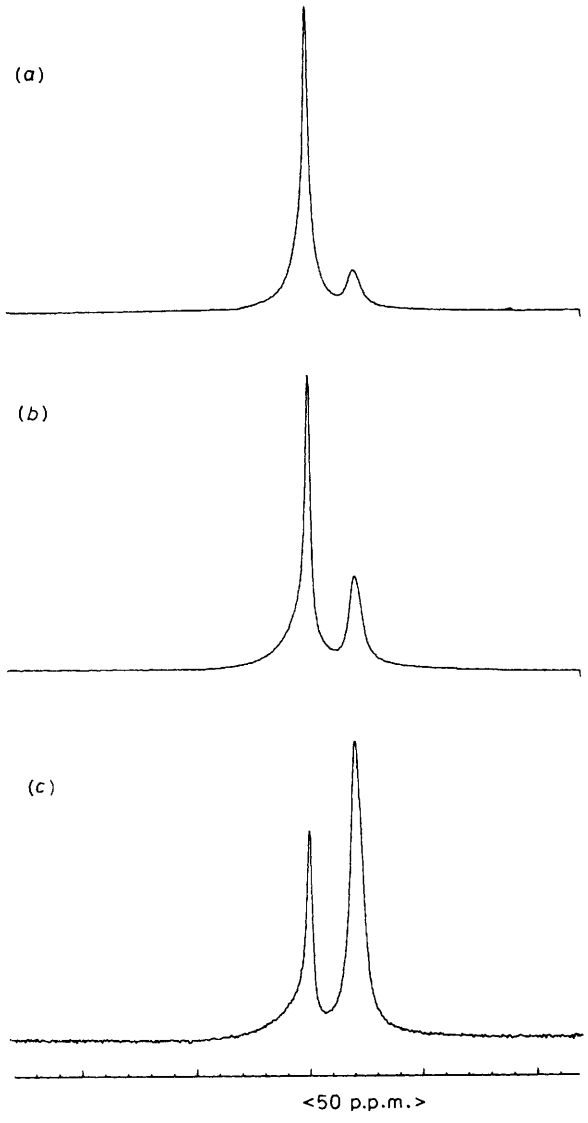

Figure 7. ^{23}Na N.m.r. spectra of 0.2 mol dm^{-3} $NaBPh_4$ with varying amounts of propeller crown (**4**): (*a*) 0.09, (*b*) 0.135, and (*c*) 0.20 mol dm^{-3} at 172 K

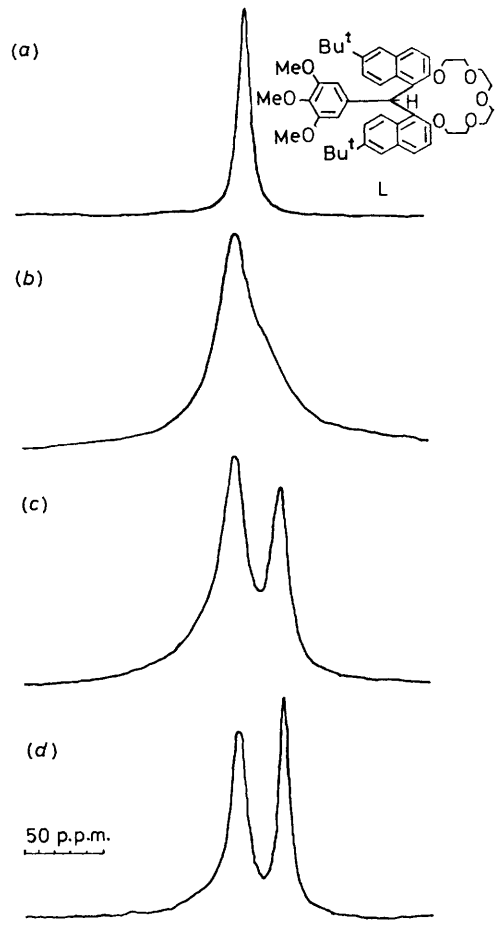

Figure 8. Variable-temperature ^{23}Na n.m.r. spectra of propeller crown (**4**) (0.129 mol dm^{-3}) and NaSCN (0.2 mol dm^{-3}) in pyridine-CD_2Cl_2 (1:1): (*a*) 300, (*b*) 208, (*c*) 182, and (*d*) 172 K

varied. In a further experiment, (*e*), an equimolar mixture of the crowns (**4**) and (**6**) was used, with an excess of $NaBPh_4$. The following deductions could be made. Increase of L:M ratio (*a*) above 0.3 gave observable amounts of the second signal, its ratio relative to the first (solvated) increasing to 2:1 for ligand (**4**) at a L:M ratio of 1.0 (and at 178 K) as shown in Figure 7. Results on several crowns (**1**)—(**6**), and (**8**) indicate that the signal appears at different temperatures and that it changes in shift for different ligands, (*b*) (Table 5), and there is proportionately more of it present in solutions of 6-donor crowns. For the asymmetrically substituted dimethyl crown (**3**), the signal appears to be multiple, apparently two overlapping peaks. This is reasonable, since at low temperatures the propeller is known to provide different proportions of the isomers differing in the orientation of the phenyl ring. In one experiment, (*c*), thiocyanate was substituted for tetraphenylborate as the counter ion; the two signals appeared in the same ratios and at the same temperatures. Drop in temperature, (*d*), caused the ratio of the unknown to the 'solvated' sodium signal to increase. Figures 7 and 8 illustrate the observations (*a*), (*c*), and (*d*) respectively. The observations under (*a*) and (*b*) show that the unknown signal is not just an aggregate of solvated cations, but must contain crown in some way. Observation (*c*) shows that it is unlikely to be associated with ion pairing, and observation (*d*) shows that a mobile equilibrium is still occurring at the lowest temperatures. Finally in experiment (*e*) (see Figure 9) we observed one extra signal in the location expected for the sodium complex of crown-5, and one in the place expected for that of the crown-6, but no further signals.

Several explanatory hypotheses occur to us at the present time: the first assumes that a 'sandwich' complex occurs at low temperatures. Another hypothesis assumes that in the 'segment i equilibria' (the *trans–gauche* swivel, described in ref. 4) if the *trans–gauche* swivel is slow relative to the formation of ML^+ [equation (1), k_1] then for a sodium complex (ML'^+) with a transient *trans* segment there are available vacant co-ordination sites; the vacant site on sodium normally co-ordinated to the now unavailable oxygen in the *trans* segment could co-ordinate to an additional pyridine; alternatively, the pyridinated (solvated) sodium could co-ordinate additionally the 'free' oxygen of a segment temporarily in the *trans* state. These suggested structures, which might even occur in the same aggregate, are depicted in Figure 10. The latter suggestions would account for the formation of the second species more readily from the crown-6, which has an additional oxygen, and, according to earlier n.m.r. evidence,[4] has both segment i portions undergoing *trans–gauche* switching, while the crown-5

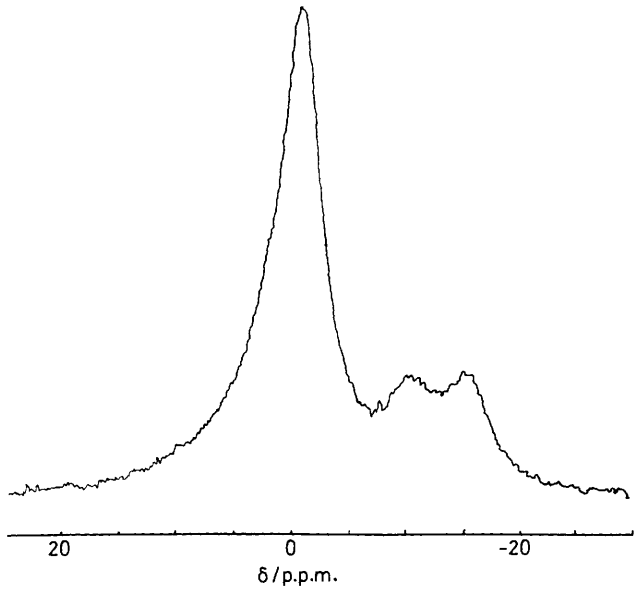

Figure 9. Low-temperature ^{23}Na signals in an equimolar mixture of propeller crowns (**4**) (0.07 mol dm^{-3}) and (**6**) (0.07 mol dm^{-3}) and 0.2 mol dm^{-3} $NaBPh_4$ in pyridine–CD_2Cl_2 (1:1) at 190 K

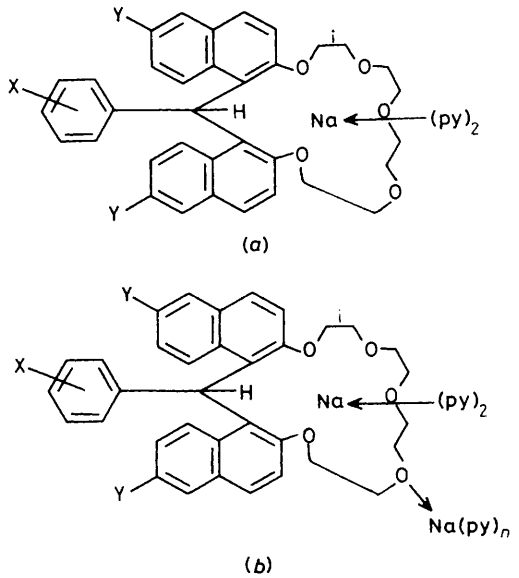

Figure 10. Possible aggregate species at low temperature: (*a*) additional pyridine co-ordinating to Na complex, (*b*) *trans* oxygen co-ordinating to 'solvated' sodium

provides only one such segment. The shift separation (see Figure 2 for example) between the two species at low temperatures may be caused by the ring current effect of the aromatic moieties of the propeller (which should be dramatically changed for the *trans* segment). It is not clear why the line for such new species would be narrow. The sandwich hypothesis is thus less likely, since it would be favoured by the crown-5 rather than the crown-6. The sandwich hypothesis was finally discarded after experiment (*e*), since a 'mixed' sandwich at an intermediate shift would have been anticipated, in addition to the other two signals. We were also able to rule out involvement of anion, since similar results were obtained for the two different salts used. Our remaining explanations are still consistent with our observations to date. A similar explanation (in terms of a *trans–gauche* equilibrium) may account for Popov's inclusive and exclusive caesium cryptates.[10] Truter's early mechanistic hypothesis for the dissociation of the dibenzo-18-crown-6 sodium complex[17] suggested a *trans–gauche* swivel as a process with a suitable magnitude of activation energy; the crystal structure of free dibenzo-18-crown-6 contains two *trans* and two *gauche* segments, yet that of the complex has all-*gauche* ether segments.

In summary, an attempt has been made to investigate sodium exchange mechanisms in solvents chosen to simulate ion-selective electrode membranes. It is seen that the exchange mechanism is largely dissociative at the operational temperatures involved in ion-selective electrodes. The exchange rate ($1/\tau$), which is the relevant one for comparison with the ion-selective electrode situation, increases in the order (**2**) $\simeq$ (**3**) < (**4**) < (**6**) < (**7**) at 240 K. The locked propeller seems to be a significant determinant of dissociation rate of Na complexes. The crystal structure gives pointers to the possible role of the counter ion BPh_4^- and to the possible co-ordination of the donor groups of the plasticisers in ion-selective electrode membranes. A new sodium-containing species has been discovered at low temperatures and hypotheses as to its structure have been made.

Acknowledgements

The S.E.R.C. is thanked for the instrumental facilities (*X*-ray and n.m.r.) used in this work, and for financial support (to M. T. and M. McD.).

References

1 Presented in part at the I.U.P.A.C. conference, Manchester, September 1985, and at the Ninth International Symposium on Macrocyclic Chemistry, Stirling, August 1984.
2 J. C. Lockhart, *J. Chem. Soc., Faraday Trans. 1*, 1986, 1161.
3 R. D. Armstrong and M. Todd, *Electrochim. Acta*, 1987, **32**, 155 and refs. therein.
4 J. C. Lockhart, M. B. McDonnell, W. Clegg, and M. N. S. Hill, *J. Chem. Soc., Perkin Trans. 2*, 1987, 639.
5 G. J. Moody, R. B. Oke, and J. D. R. Thomas, *Analyst (London)*, 1970, **95**, 910.
6 E. Shchori, J. Jagur-Grodzinski, and M. Shporer, *J. Am. Chem. Soc.*, 1971, **93**, 7133.
7 E. Shchori, J. Jagur-Grodzinski, and M. Shporer, *J. Am. Chem. Soc.*, 1973, **95**, 3842.
8 M. Shporer and Z. Luz, *J. Am. Chem. Soc.*, 1975, **97**, 665.
9 P. Szczygiel, M. Shamsipur, K. Hallenga, and A. I. Popov, *J. Phys. Chem.*, 1987, **91**, 1252.
10 E. Schmidt and A. I. Popov, *J. Am. Chem. Soc.*, 1983, **105**, 1873.
11 A. Delville, H. D. H. Stover, and C. Detellier, *J. Am. Chem. Soc.*, 1987, **109**, 7293.
12 G. M. Sheldrick, SHELXTL and SHELX 86, University of Göttingen, 1986; W. Clegg, *Acta Crystallogr., Sect. A*, 1981, **37**, 22.
13 W. Hong and B. E. Robertson, 'Structure and Statistics in Crystallography,' ed. A. J. C. Wilson, Adenine Press, New York, 1985, p. 125.
14 'International Tables for *X*-Ray Crystallography,' Kynoch Press, Birmingham, 1974, vol. 4, pp. 99, 149.
15 W. Clegg and J. C. Lockhart, *J. Chem. Soc., Perkin Trans. 2*, 1987, 1621.
16 J. C. Lockhart, M. B. McDonnell, and W. Clegg, *J. Chem. Soc., Chem. Commun.*, 1984, 365.
17 M. R. Truter, quoted in ref. 6.

Received 12*th November* 1987; *Paper* 7/2010